

PHYSICAL REVIEW D

PARTICLES AND FIELDS

THIRD SERIES, VOLUME 38, NUMBER 3

1 AUGUST 1988

Spin-parameter measurements in Λ and K_S production

B. E. Bonner, J. A. Buchanan, J. M. Clement, M. D. Corcoran, J. W. Kruk,
H. E. Miettinen, R. M. Moss, G. S. Mutchler, F. Nessi-Tedaldi, M. Nessi,
G. C. Phillips, J. B. Roberts, P. M. Stevenson, and S. R. Tonse

T. W. Bonner Laboratories, Physics Department, Rice University, Houston, Texas 77251

A. Birman, S. U. Chung, R. C. Fernow, H. Kirk, and S. D. Protopopescu
Physics Department, Brookhaven National Laboratory, Upton, New York 11973

T. Hallman and L. Madansky

Department of Physics and Astronomy, Johns Hopkins University, Baltimore, Maryland 21218

B. W. Mayes and L. S. Pinsky

Physics Department, University of Houston, Houston, Texas 77004

Z. Bar-Yam, J. Dowd, W. Kern, and E. King

Department of Physics, Southeastern Massachusetts University, North Dartmouth, Massachusetts 02747

(Received 18 February 1988)

The Brookhaven Alternating Gradient Synchrotron polarized proton beam incident on a beryllium target was used for inclusive Λ production at beam momenta of 13.3 and 18.5 GeV/c. The beam polarization was transverse to the beam direction with magnitude 0.63 at 13.3 GeV/c and 0.40 at 18.5 GeV/c. The Λ polarization was measured and found to be in agreement with results from earlier experiments which used unpolarized proton beams. Analyzing power A_N and spin transfer D_{NN} of the Λ 's were both measured and compared with a hyperon-polarization model in which the polarization arises from a Thomas-precession effect. There is good agreement with its predictions: $A_N=0$ and $D_{NN}=0$. In particular, our measurement of $\langle D_{NN} \rangle = -0.009 \pm 0.015$ supports the idea that the valence quarks carry all of the hadron spin, since this assumption is implicit in the model's use of SU(6) wave functions to form final-state hadrons from beam fragments and sea quarks. The presence of substantial K_S samples at both beam momenta and $\bar{\Lambda}$'s at 18.5 GeV/c prompted a measurement of their analyzing powers, which yielded $A_N(K_S) = -0.094 \pm 0.012$ at 13.3 GeV/c beam momentum and -0.076 ± 0.015 at 18.5 GeV/c, and $A_N(\bar{\Lambda}) = 0.03 \pm 0.10$.

INTRODUCTION

The measurement of a significant polarization in inclusive Λ (1116 MeV/c²) production using a 300-GeV/c unpolarized proton beam on a beryllium target¹ rekindled interest in spin as a factor influencing the outcome of high-energy reactions. Previous expectations were that spin effects would die out at higher energies, since the large multiplicity of final states makes it unlikely to have the coherent interference between amplitudes that leads to polarization effects. The Λ polarization was observed along the direction normal to the production plane defined by $\mathbf{p}_{\text{beam}} \times \mathbf{p}_\Lambda$. This is the only axis along which polarization is permitted since the Λ is produced by the

strong interaction in which parity is conserved. Data taken at different beam energies show that the polarization has the following characteristics: (a) It is roughly independent of center-of-mass energy; (b) it increases monotonically with both Feynman x (x_F) and transverse momentum (p_T), saturating at a value $p_T \sim 1$ GeV/c; and (c) it is only weakly dependent on target type, decreasing with increasing atomic weight.²

Since perturbative QCD is not expected to be applicable in this region of energy and transverse momentum, we discuss phenomenological models which use static quark wave functions. In the naive quark model the Λ is composed of a single quark of each of the flavors u , d , and s . The SU(6) wave function always has the ud quark system in a spin-singlet state. As a consequence the Λ

polarization is the same as that of the s quark. Hence, the s quark is either produced polarized or else acquires it during recombination with the incident baryon fragment. Andersson, Gustafson, and Ingelman³ (Lund model) and DeGrand and Miettinen⁴ (DM) both venture semiclassical arguments for the Λ polarization but offer differing mechanisms by which the s quark is polarized. In both models the incident beam proton is treated as a (ud) diquark system plus a single u quark. The diquark continues forward with its flavor and spin state unchanged and picks up an s quark from the sea to form the final state Λ .

In the Lund model, a color dipole field confined to one dimension stretches between the diquark D and the central collision region C (Fig. 1). Angular and transverse momentum are assumed to be locally conserved in this field. In the $s\bar{s}$ pair formed in the field the two quarks have equal and opposite transverse momenta k_T with respect to the axis CD , which results in an orbital angular momentum \hat{m} . To compensate for this the spins of the $s\bar{s}$ pair are oriented in the opposite direction. Thus, there is a correlation established between the direction of k_T of the s quark and its spin. The polarization arises from a “trigger-bias” effect; i.e., we ask for events of a certain p_T and since the cross section of the diquark falls with p_T it is more probable that the k_T of the s quark contributes to total p_T (as in Fig. 1) than detracts from it. This model does not allow for the polarizing of beam valence quarks during the interaction, e.g., as in $K^-p \rightarrow \Lambda + X$, in which the Λ 's are observed to have a large polarization.⁵

In the DM model polarization originates from Thomas precession, the result of this being that sea quarks which are accelerated in the transition from the sea to the final state preferentially recombine with their spins down with respect to $\mathbf{p}_{\text{beam}} \times \mathbf{p}_\Lambda$ while valence quarks from the incident baryon (which are decelerated) tend to have their spins up. In addition to proposing a polarization mechanism, DM also provide a general framework for computing polarization observables in terms of polarization effects at the quark level, using SU(6) wave functions. This framework is only applicable for the forward-scattering region, since it assumes that the final-state particle receives as many valence quarks as possible from the beam particle. The model is not limited to Λ production and makes predictions for all of the $\frac{1}{2}^+$ octet baryons. Subsequent polarization measurements of inclusive Σ^+ (Ref. 6), Σ^0 (Ref. 7), Σ^- (Ref. 8), Ξ^0 (Ref. 9), and Ξ^- (Ref. 10) production showed good general agreement with the model. The DM framework also allows one to make pre-

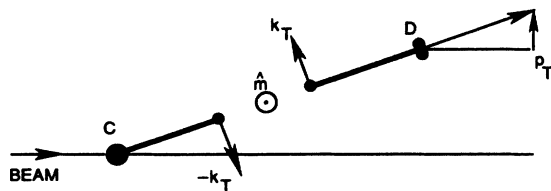


FIG. 1. Polarization mechanism of the Lund model. C denotes collision region. D denotes scattered diquark. The produced $q\bar{q}$ pair have equal and opposite transverse momenta $\pm k_T$ which generate an orbital angular momentum \hat{m} .

dictions for spin observables other than P , viz., analyzing power A_N and depolarization D_{NN} which require polarized beams. Measurements of these parameters, particularly D_{NN} for which the prediction is parameter-free, provide crucial tests of the model and its assumption that the process can be treated at the quark level. A more detailed discussion of the model is presented in Sec. III C.

We measured P , A_N , and D_{NN} for the reaction $p + \text{Be} \rightarrow \Lambda + X$ at beam momenta of 13.3 and 18.5 GeV/c, collecting 321 000 and 243 000 Λ 's, respectively, observed through their dominant decay mode $\Lambda \rightarrow p\pi^-$. The Brookhaven Multiparticle Spectrometer (MPS) was used to trace the tracks of the Λ decay products. The Λ polarization was extracted by measuring the asymmetry in the angular distribution resulting from the parity-violating weak decay. The angular distribution of the decay proton in the Λ rest frame is given by

$$\frac{dN}{d(\cos\theta^*)} = N(1 + \alpha P_\Lambda \cos\theta^*), \quad (1)$$

where P_Λ is the magnitude of Λ polarization and θ^* is the angle between the polarization axis and the decay proton momentum in the Λ rest frame. The parameter α is a measure of the interference between s and p waves of the final state and has been measured to be 0.645 ± 0.017 (Ref. 11). We follow the usual set of conventions¹² to describe the polarization parameters (Fig. 2) described by \hat{L} along the direction of motion of the particle, \hat{N} normal to the scattering plane in a direction $\mathbf{p}_{\text{beam}} \times \mathbf{p}_\Lambda$, and \hat{S} in the scattering plane defined by $\hat{S} = \hat{N} \times \hat{L}$. (Lower-case \mathbf{p} is used to indicate momenta.) P_Λ is measured with respect to \hat{N} . A_N is proportional to the left-right production asymmetry about the beam polarization vector. Depolarization D_{NN} is a measure of \hat{N} component polarization transfer from the incident beam particle to the forward scattered Λ .

In Sec. II we describe the experimental setup, viz., polarized beam, the spectrometer and associated detectors, the trigger, and the measurement of beam polarization. Section III covers the data analysis, event reconstruction, acceptance correction, evaluation of spin parameters, and a comparison of Λ data to theory. Section IV describes the K_S and $\bar{\Lambda}$ analysis.

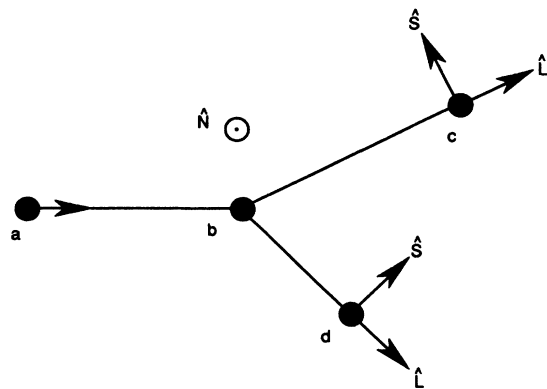


FIG. 2. Spin-parameter subscript definitions according to the Ann Arbor spin-parameter convention, showing an interaction $a + b \rightarrow c + d$ in the laboratory frame. \hat{N} points out of the page.

II. EXPERIMENTAL PROCEDURE

The experiment was conducted at the Brookhaven Alternating Gradient Synchrotron (AGS). Preliminary results from this run are presented in Ref. 13.

A. Acceleration of polarized protons

Polarized protons were produced in a 25- μ A H^- ion source, preaccelerated to 200 MeV in the Linac and then injected into the AGS main ring.¹⁴ During acceleration the protons experienced the usual effects of the vertical magnetic fields, which caused them to precess about the vertical axis with frequency $\omega_p = G\gamma\omega_c$. Here $G = (g - 2)/2$ which is 1.79 for the proton, γ is the Lorentz energy factor defined by (beam energy)/(proton mass) and ω_c is the cyclotron frequency. This precession did not change the projection S_z of the spin vector on the vertical axis and so the polarization was not affected. However, the horizontal focusing fields did tend to deflect the polarization away from the vertical. The proton "sees" these fields at frequencies $\omega_{HF} = (kP \pm \nu)\omega_c$ (Ref. 15), where $K = 1, 2, 3, \dots$, P reflects the symmetry of the accelerator and depends on the number of magnets in the ring, and ν is the betatron tune of the accelerator. Normally the deflection to the spin tends to be canceled out in successive orbits since the proton's spin precession about the vertical axis causes it to be more or less randomly aligned each time it encounters a horizontal field. However, when the resonance condition $\omega_p = \omega_{HF}$ occurs, i.e., $G\gamma = (kP \pm \nu)$, the deflections add constructively and the beam is depolarized in a short time. About 40 such depolarizing resonances had to be passed when accelerating the beam up to 18.5 GeV/c. This problem was countered by use of 10 fast-pulsed quadrupole and 95 dipole magnets installed in the ring specifically for this purpose. Pulsing the quadrupoles changed the focusing fields which shifted the betatron tune. By doing this just as the beam energy reached a resonance value the resonance condition was changed and so no depolarization occurred.

Polarization of the injected, accelerated, and extracted beams was monitored by 3 polarimeters in the 200-MeV Linac, the main ring and the neighboring extracted beam line, respectively. A fourth polarimeter was situated just upstream of our experiment (see Sec. II C) but this was not used by the AGS for polarization monitoring. The 200-MeV polarimeter¹⁶ was placed between the Linac and the main ring and consisted of two independent polarimeters each having a left and a right arm. Polarization was extracted by measuring the left-right asymmetry of scattering from a carbon string in the beam line. Typical beam polarization at this stage was $\sim 75\%$. The polarimeter in the main ring was used only during the setup of the polarized beam, at which time the pulsed quadrupole timings and strengths had to be fixed so as to neutralize the depolarizing resonances. The University of Michigan polarimeter¹⁶ in the adjacent beam line was an absolute polarimeter in the sense that it was not calibrated against any other polarimeter but rather by the use of

a polarized target. There was a forward arm and recoil arm on each side to detect the forward and recoil particles, each arm being a magnetic spectrometer. The main ring polarimeter and the polarimeter belonging to our experiment were calibrated against this polarimeter.

B. Experimental apparatus and trigger

The experiment was performed with typical beam intensities of 1.8×10^{10} protons/pulse (800 msec) in the AGS ring and $(2.5 - 3.0) \times 10^6$ protons/pulse incident on our target. The target was a beryllium cylinder 4 cm long and 4 cm in diameter, providing a compact source of Λ 's. Using an equivalent LH_2 target would have greatly complicated the establishment of the Λ decay volume. Another reason for using beryllium was to facilitate comparison with existing P_Λ data¹⁷ (unpolarized beam), since many previous experiments used Be targets. Our main detector was the Brookhaven Multiparticle Spectrometer (MPS) (Ref. 18) which has an array of 52 wire-chamber planes inside a C magnet 457 cm long by 183 cm wide, with a 122-cm gap between the horizontal pole faces (Fig. 3). A homogeneous 5-kG magnetic field was maintained between the pole faces in the upward vertical direction bending positive particles towards the right. The beam height was midway between the pole faces, so that the whole experimental arrangement was symmetric about the horizontal plane. In order to reject Λ 's with $p_T < 0.5$ GeV/c, below which polarization has been observed to be small, the beam and the target were offset horizontally by 134.5 cm with respect to the MPS central axis. This removed Λ 's produced with a scattering angle $< 5.5^\circ$ in the laboratory from the MPS acceptance. Another reason for this offset was to avoid having the beam pass through the live area of the wire chambers. A polarimeter viewing the target to measure the beam polarization will be described in Sec. II C. Scintillators S_2 (1.4 cm diam) and S_3 (veto counter with a 1.4-cm diam-aperture) immediately upstream of the target ensured that the interaction was caused by a beam particle, and also vetoed interactions caused by the beam halo. The count of $S_2 \cdot S_3$ was used to define the beam rate. The Λ decay volume was defined by scintillators S_4 and S_5 placed between the target and the MPS. A produced Λ would pass through S_4 (veto) but decay upstream of S_5 . The Λ decay products (p, π^-) were then required to register at least a double minimum ionizing pulse height in S_5 . This region was far enough from the spectrometer magnet for us to ignore the mag-

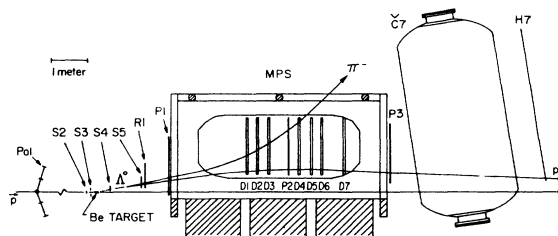


FIG. 3. Plan view of the experimental setup.

netic field, and no correction for precession of the Λ spin was necessary. A three-coordinate proportional wire chamber (PWC) $R1$ was placed downstream of $S5$ to aid in vertex reconstruction by providing hit coordinates as close as possible to the decay region.

Multiplicity information (number of clusters) from the PWC's ($P1, P2, P3$) could be read out by hardware and was used in the second stage of the trigger. Immediately downstream of the MPS magnet were the Cherenkov counter $C7$ and scintillator hodoscope $H7$, both subdivided into matching segments. This made it possible for triggering purposes to detect coincidences/anticoincidences between the two detectors in any particular segment. $C7$ was set to a threshold of $\beta\gamma \approx 15$ which corresponded to a proton of 14.1 GeV/c or a pion of 2.1 GeV/c. The Λ trigger used only scintillator pulse heights, PWC multiplicity information, and a $C7 \cdot H7$ anticoincidence requirement. Track reconstruction was provided by the PWC's ($P1, P2, P3$) and drift chambers ($D1$ to $D7$) located inside the MPS magnet but no track information was used in the trigger, so as to minimize any influence it might have on the Λ polarization measurement. A summary of this simple trigger follows.

(i) Λ 's were constrained to decay between $S4$ and $S5$.

(ii) The minimum multiplicity requirements of 2, 2, and 1 on $P1$, $P2$, and $P3$, respectively, ensured that the relatively low momentum π^- (1–1.5 GeV/c) passed through at least three drift chambers and two PWC's, and they also enhanced collection of forward-scattered ($x_F > 0$) Λ 's by triggering on high-momentum protons (note: $\mathbf{p}_\Lambda \approx \mathbf{p}_{\text{proton}}$) that traversed the entire magnet length. An upper limit of 5 was put on the multiplicities of $P1$, $P2$, $P3$ to reject events containing photon showers, as it was impossible to isolate and reconstruct tracks from these events.

(iii) The $\overline{C7} \cdot H7$ anticoincidence suppressed pions from events with K_S decay which could otherwise have met all trigger requirements.

Data acquisition was performed with the MPS's CAMAC and FASTBUS (Ref. 19) systems and written to tape by a VAX 11/750 at a rate of ≈ 35 triggers/spill. The use of the Online Data Facility's (OLDF) VAX 8600 enabled us to monitor constantly wire-chamber hit patterns, analog-to-digital-converter (ADC) spectra, beam and trigger rates, and also to reconstruct events and calculate physical observables. Approximately 5% of all recorded events were monitored in this fashion.

C. The beam-polarization measurement

The transverse vertical component of beam polarization was measured at 13.3 GeV/c by a polarimeter consisting of a pair of three scintillator telescopes in the horizontal plane viewing the beryllium target. During the 18.5 GeV/c run the Be target was left alone but the polarimeter was moved further upstream and instead viewed a polyethylene target, which because of its larger analyzing power allowed for a more accurate measurement of polarization. Two vertical arms were added to the polarimeter to also measure the horizontal transverse component of polarization which occurred as a result of

vertical bends in the extracted beam line. The polarimeter measured the left versus right asymmetry of elastic scattering of the beam particle by detecting the recoil particle. We required a coincidence between the three scintillators in an arm, with minimum-ionizing thresholds in the first two scintillators and a large signal from the third, indicating that the particle had stopped on it. The absolute polarimeter in the next beam line was used for calibration from which we determined the analyzing power of our polarimeter at 13.3 (18.5) GeV/c to be 0.00900 ± 0.00025 (0.0124 ± 0.0048).

The sign of the beam polarization was reversed for each spill so as to make measurements of A_N and D_{NN} more independent of systematic influences. At the end of a run, four scalers were obtained, one for each arm (L or R) and for each sign (+ or -) of beam polarization. Polarization was calculated using

$$P_B = \frac{1}{\text{analyzing power}} \frac{1-r}{1+r}, \quad (2)$$

where

$$r = \left[\frac{L^- R^+}{R^- L^+} \right]^{1/2}. \quad (3)$$

This method²⁰ has the advantage that it is independent (to first order) of differences in efficiency, solid angle, and errors in alignment between the two polarimeter arms. However, P_B cannot be obtained separately for "spin-up" spills and "spin-down" spills, instead we have to average the two and assume $P_B(\text{up}) = -P_B(\text{down})$. Information from the 200-MeV polarimeter in the Linac showed that there was not much variation between the two. In any case A_N and D_{NN} are independent to first order of a difference between the magnitudes of spin-up and spin-down beam polarization. Averaged over all runs the vertical component of beam polarization at 13.3 (18.5) GeV/c was 0.63 (0.36), and the transverse horizontal component (x) measured at 18.5 GeV/c was 0.18.

III. DATA ANALYSIS

A. Event selection

The data analysis was done using the mainframe CDC 7600 at the Brookhaven Central Scientific Computing Facility (CSCF), where decoding, tracking, and vertex reconstruction was performed. During this first pass through the data all events with at least one vertex formed by a pair of oppositely charged particles were written to output summary tape. The background contamination of this sample came from three major sources.

(a) Interactions which occurred far enough downstream of the Be target that the veto counter $S4$ could no longer eclipse $S5$. These were removed by (i) applying cuts requiring the vertex to be within the fiducial decay volume defined by $S4$ and $S5$ and (ii) target pointing cuts requiring the vector $\mathbf{p}_{\text{parent}} = \sum \mathbf{p}_{\text{daughters}}$ to project back to the target. Figure 4 shows the invariant-mass distribution of events passing these vertex and target cuts, calculated under the hypothesis $\Lambda \rightarrow p\pi^-$. The mean and full

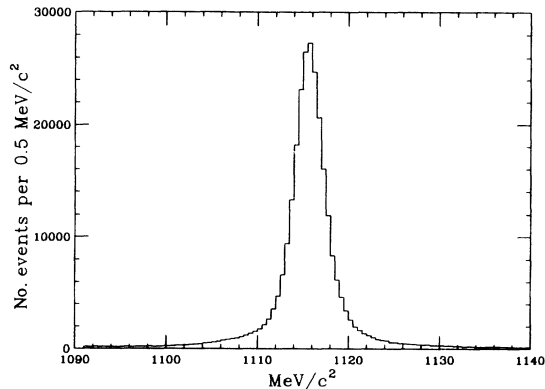


FIG. 4. Invariant mass (m_Λ) of the Λ data after cuts, using the $\Lambda \rightarrow p\pi^-$ hypothesis.

width at half maximum (FWHM) of this m_Λ distribution were 1115.6 and 4.7 MeV/c², respectively, and the background under the peak was estimated to be 0.5%.

(b) Weakly decaying particles with $c\tau$ comparable to that of the Λ , mainly K_S . Figure 5 shows the same event sample as in Fig. 4 but with invariant mass m_{K_S} calculated under the $K_S \rightarrow \pi^+\pi^-$ hypothesis. The majority of Λ events have $m_{K_S} < 400$ MeV/c² and so do not appear on the plot. The Λ/K_S ambiguous events were resolved in favor of Λ since (i) no evidence of a K_S peak remains when a cut of $1110 < m_\Lambda < 1122$ MeV/c² is applied (dotted line in Fig. 5) and (ii) K_S 's are suppressed by the $\overline{C7}\cdot H7$ trigger requirement.

(c) Λ events in which the invariant mass fell outside the peak. This occurred whenever one of the decay particle momenta was incorrectly determined, usually because of missing hits in the upstream wire chambers. The resulting m_Λ was within 100 MeV/c² from the true value.

Another source of contamination which appeared within the Λ invariant-mass peak rather than the background came from Λ 's produced by the decay of Σ^0 and Ξ^0 . The majority of these are from $\Sigma^0 \rightarrow \Lambda\gamma$, since Ξ^0 production is only $\sim 1\%$ of inclusive Λ production.²¹ The ratio of production of Σ^0 to prompt Λ in

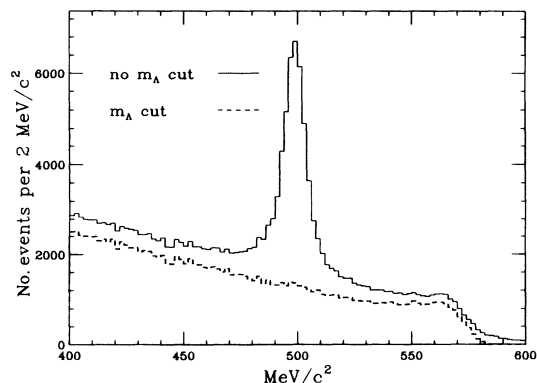


FIG. 5. Invariant mass (m_{K_S}) of the Λ data using the $K_S \rightarrow \pi^+\pi^-$ hypothesis, both before and after a cut on m_Λ .

$p + \text{Be} \rightarrow \Sigma^0 + X$ and $p + \text{Be} \rightarrow \Lambda + X$ at 28.5 GeV/c has been measured²² as a function of p_T . Weighting this data with our observed p_T distribution we estimate the ratio between Σ^0 and directly produced Λ to be 0.386 ± 0.041 . It is unfortunate that we cannot isolate the Λ 's from Σ^0 decay, since some of the Σ^0 polarization is carried over to the Λ . This will be discussed later in more detail.

A total of 321 000 (243 000) events at 13.3 (18.5) GeV/c passed vertex and target cuts, as well as an invariant-mass cut of $1110 < m_\Lambda < 1122$ MeV/c² and were taken to be bonafide Λ 's. The trigger condition favored forward produced Λ [$\langle x_F \rangle = 0.27$ (0.18)] of moderately high p_T [$\langle p_T \rangle = 0.9$ (1.0) GeV/c] at 13.3 (18.5) GeV/c. Mean Λ energy in the laboratory was 6.0 (6.7) GeV. The kinematic range in x_F and p_T over which events were collected is shown in Fig. 6. The region was subdivided into 10 bins and the polarization parameters P , A_N , and D_{NN} were calculated for each bin.

B. Calculation of P , A_N , and D_{NN}

Polarization P is obtained from the $\cos\theta^*$ distribution where θ^* is the angle (in the Λ rest frame) between the decay proton momentum vector and the polarization axis defined by $\mathbf{p}_{\text{beam}} \times \mathbf{p}_\Lambda$. For a data sample free of any acceptance bias the expected distribution is of the form

$$f^0(\cos\theta^*) = \frac{N}{2}(1 + \alpha P_\Lambda \cos\theta^*), \quad (4)$$

where N is the total number of events, $\alpha = 0.645 \pm 0.017$, and P_Λ is the magnitude of the polarization. Given such a distribution

$$P_\Lambda = \frac{2}{\alpha} \left[\frac{N_2 - N_1}{N_2 + N_1} \right], \quad (5)$$

where

$$N_1 = \int_{-1}^0 f^0(\cos\theta^*) d(\cos\theta^*) \quad (6)$$

and

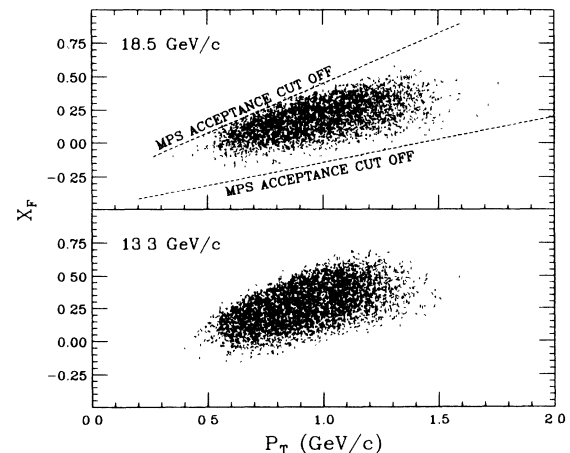


FIG. 6. Acceptance domain of Λ data after all cuts, as a function of p_T and x_F , and indicating the limits of acceptance.

$$N_2 = \int_0^1 f^0(\cos\theta^*) d(\cos\theta^*) . \quad (7)$$

The ideal distribution $f^0(\cos\theta^*)$ can be influenced by a number of factors. Some of these bias the data if the apparatus is asymmetric about the horizontal plane. Since we measure P_Λ by comparing decay protons above versus those below the decay plane (which is close to the horizontal plane) we could obtain a false value of polarization. In particular, this problem could be caused by asymmetric detector efficiencies (not only for the spectrometer but also other parts like *C7* and *H7*) or by the beam not being incident horizontally at the midplane of the MPS. From our data we determined that the beam was incident 0.5 cm above the midplane. The possible consequences of this were studied by first generating Monte Carlo events symmetrically about the midplane and then generating the same events with the mean interaction position raised by 0.5 cm. This was checked for three kinematic regions over the range x_F 0.0–0.45. No significant change in P_Λ was seen between the two cases, implying that the polarization was insensitive to such a small effect.

Asymmetries caused by detector efficiencies would be reflected in the distribution of the azimuthal angle ϕ of the Λ 's p_T vector about the beam axis. [Note: $\tan(\phi) = p_y/p_x$.] For a perfectly symmetric sample we should have $\langle\phi\rangle = 0$. In our data the value of $\langle\phi\rangle$ fluctuated about zero for the different p_T and x_F bins. Reproducing these values with the Monte Carlo events once again made no change in P_Λ . Therefore, we can safely say that the data is free of significant asymmetries about the midplane.

There is, however, another effect which changes the value of P_Λ even for symmetric detectors. The event losses appear in the $\cos\theta^* = 0$ region for high- x_F events [Fig. 7(a), upper plot] or the $\cos\theta^* = \pm 1$ region for low- x_F events [Fig. 7(b), lower plot]. Monte Carlo-generated events were used to reproduce and understand the source of these losses. The Monte Carlo program generated Λ 's

according to input p_T and x_F distributions similar to those seen in the data and tracked the Λ decay products through the MPS magnetic field. The trigger requirements were the same as those imposed on the data. The causes for these losses can be understood by first considering those Λ 's that are produced in the horizontal plane. Since the detector size and position limits the momentum p_Λ to have $\pm 3.5^\circ$ elevation with respect to the horizontal plane in the laboratory frame we can say that all Λ 's are in this plane. Then an event with $\cos\theta^* = 1(-1)$ would have the decay proton emitted vertically upward (downward) in the laboratory frame and the π^- emitted vertically downward (upward), whereas a $\cos\theta^* = 0$ event would have a horizontal decay. Λ 's with high x_F and low p_T have small production angles and so pass close to the edges of the wire chambers. For these events a "horizontal" decay often results in one daughter particle being lost in a chamber frame or failing to reconstruct due to a lack of hits. In contrast with this, low- x_F regions (for which the decay event from the slow Λ have a wider opening angle in the laboratory) suffer greater event losses at $\cos\theta^* = +1(-1)$ caused by the upper (lower) edges of the wire chambers. The similarity between the Monte Carlo event and data distributions in Fig. 7(a) shows that the Monte Carlo program accounts for event losses fairly accurately. Taking the true P_Λ to be given by Eq. (5) we see that a symmetric acceptance loss would decrease N_1 and N_2 by about the same amount. Therefore, the numerator in Eq. (5) is unchanged but the denominator has been decreased. This is corrected by determining the efficiency $E(\cos\theta^*)$ from the Monte Carlo events, and then correcting the data by the same amount. In order to average out any bin-to-bin statistical fluctuations in the $\cos\theta^*$ distribution of the Monte Carlo events, $E(\cos\theta^*)$ is parametrized as

$$E(x) = a + bx^2 + cx^4 + dx^6 , \quad (8)$$

where $x = E(\cos\theta^*)$. (Only even terms of x are included since the detector is symmetric.) The parameters a , b , c , and d are then adjusted to give a best fit to $E(\cos\theta^*)$ and the resulting function is then used to correct P_Λ . After the correction we found that this effect altered the true P_Λ by less than 3% for all kinematic regions. This was either smaller or roughly equal to the statistical error on P_Λ , and so the plotted data have not been corrected. In the low- x_F kinematic regions the agreement between Monte Carlo program and data was not very good. Here the efficiency for accepting an event was much lower ($\approx \frac{1}{30}$) than for the higher- x_F regions. The measured P_Λ was not corrected for those $\cos\theta^*$ distributions since we could not expect to reproduce the original distribution given only 1 event out of 20 or 30. Since the efficiency affects spin-up and spin-down beam events equally this does not affect our measurements of A_N and D_{NN} . We also add that the uncorrected P_Λ data agrees well with data for other experiments. Additional information regarding the analysis and Monte Carlo corrections can be found in Ref. 23.

The final values of P_Λ as a function of x_F are shown in Fig. 8 and summarized in Table I. The sign of P_Λ is neg-

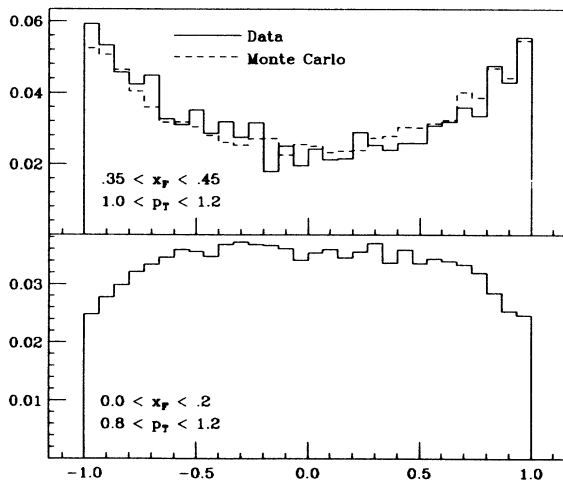


FIG. 7. $\cos\theta^*$ distribution of data and Monte Carlo events in different kinematic regions.

ative with respect to $\mathbf{p}_{\text{beam}} \times \mathbf{p}_\Lambda$ and the magnitude increases monotonically with x_F up to $P_\Lambda \simeq 30\%$ at $x_F=0.5$. These results are in excellent agreement with those of earlier unpolarized-beam $p + \text{Be} \rightarrow \Lambda + X$ experiments some of which are shown in the figure.

Analyzing power A_N , the ratio of the left-right scattering asymmetry and the beam polarization, is given by

$$A_N(\phi) = \frac{1}{P_B \cos\phi} \left[\frac{N^L(\phi) - N^R(\phi)}{N^L(\phi) + N^R(\phi)} \right], \quad (9)$$

where $P_B \cos\phi = \mathbf{P}_B \cdot \hat{\mathbf{N}}_\Lambda$ is the effective component of the beam polarization relative to the Λ scattering plane, where $\tan\phi = p_y/p_x$. Since left scatters for spin-up beam

are equivalent to right scatters for spin down, and the MPS only accepts left scatters, we can rewrite the previous equation as

$$A_N(\phi) = \frac{1}{P_B \cos\phi} \left[\frac{N^+(\phi) - N^-(\phi)}{N^+(\phi) + N^-(\phi)} \right]. \quad (10)$$

N^+ and N^- are the numbers of Λ 's produced with beam up and down, respectively. They have been normalized to the slightly different up and down beam fluxes, and dead-time corrections have also been made even though the beam intensities are equal up to one part in 10^5 . A weighted sum of $A_N(\phi)$ is taken over the various bins of ϕ to get A_N . The resulting value of A_N is independent of

TABLE I. Λ spin observables at 13.3- and 18.5-GeV/c incident momentum.

x_F	$\langle x_F \rangle$	p_T (GeV/c)	$\langle p_T \rangle$ (GeV/c)	P	A	D_{NN}
18.5 GeV/c						
-1.0 to 0.0	-0.08	0.0 to 0.8	0.62	0.008	-0.013	-0.038
				± 0.025	± 0.023	± 0.088
-1.0 to 0.0	-0.05	0.8 to 3.0	0.98	-0.005	-0.011	+0.027
				± 0.033	± 0.030	± 0.117
0.0 to 0.2	0.09	0.0 to 0.8	0.68	-0.032	-0.009	-0.041
				± 0.016	± 0.015	± 0.040
0.0 to 0.2	0.12	0.8 to 1.2	0.96	-0.039	-0.022	-0.009
				± 0.013	± 0.012	± 0.033
0.0 to 0.2	0.13	1.2 to 3.0	1.36	-0.028	-0.015	-0.042
				± 0.028	± 0.025	± 0.073
0.2 to 0.35	0.26	0.0 to 1.2	0.99	-0.101	-0.023	-0.012
				± 0.013	± 0.012	± 0.029
0.2 to 0.35	0.28	1.2 to 3.0	1.38	-0.123	-0.042	0.039
				± 0.021	± 0.019	± 0.051
0.35 to 0.45	0.39	0.0 to 1.2	1.10	-0.145	-0.010	-0.092
				± 0.031	± 0.028	± 0.067
0.35 to 0.45	0.40	1.2 to 3.0	1.39	-0.139	0.038	0.097
				± 0.027	± 0.024	± 0.062
0.45 to 1.00	0.51	all p_T	1.43	-0.300	0.005	-0.014
				± 0.032	± 0.029	± 0.069
13.3 GeV/c						
-1.0 to 0.0	-0.08	0.0 to 0.8	0.61	-0.078	-0.010	-0.028
				± 0.029	± 0.015	± 0.066
-1.0 to 0.0	-0.05	0.8 to 3.0	0.94	0.024	-0.072	-0.005
				± 0.051	± 0.026	± 0.125
0.0 to 0.2	0.12	0.0 to 0.8	0.67	-0.028	-0.032	-0.045
				± 0.015	± 0.007	± 0.023
0.0 to 0.2	0.12	0.8 to 1.2	0.95	-0.036	-0.021	-0.009
				± 0.016	± 0.008	± 0.027
0.0 to 0.2	0.14	1.2 to 3.0	1.32	-0.095	0.022	0.018
				± 0.052	± 0.027	± 0.088
0.2 to 0.35	0.27	0.0 to 1.2	0.87	-0.087	-0.021	-0.006
				± 0.010	± 0.005	± 0.013
0.2 to 0.35	0.28	1.2 to 3.0	1.34	-0.077	0.007	-0.025
				± 0.030	± 0.015	± 0.044
0.35 to 0.45	0.40	0.0 to 1.2	0.95	-0.159	-0.014	-0.024
				± 0.014	± 0.007	± 0.018
0.35 to 0.45	0.40	1.2 to 3.0	1.35	-0.173	0.009	0.001
				± 0.033	± 0.017	± 0.045
0.45 to 1.00	0.53	all p_T	1.12	-0.218	-0.011	-0.027
				± 0.014	± 0.007	± 0.017

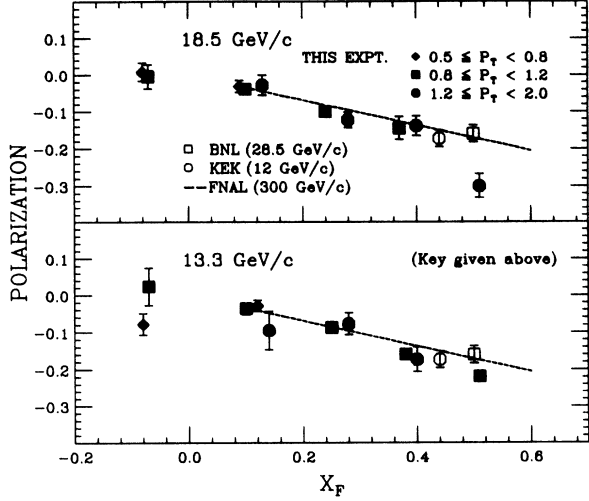


FIG. 8. Λ polarization as a function of x_F . For clarity in viewing, data points with $0.8 \leq p_T < 1.2$ GeV/c have been shifted to the left by $x_F = 0.02$.

x_F (Fig. 9), but shows a slight p_T dependence (Fig. 10) which approaches the theoretical prediction of DM at higher p_T .

We also measured A_S , the analyzing power for the component of beam polarization in the scattering plane. Since Λ production is by the strong interaction in which parity is conserved, this is expected to be zero. We observed $A_S = -0.003 \pm 0.005$, a value that is consistent with zero.

Depolarization (D_{NN}) is a measure of the transfer of polarization during the transition, in this case between the \hat{N} components of beam and Λ polarization. A depolarization of zero indicates that the spin of the final state Λ is independent of the initial proton polarization, while

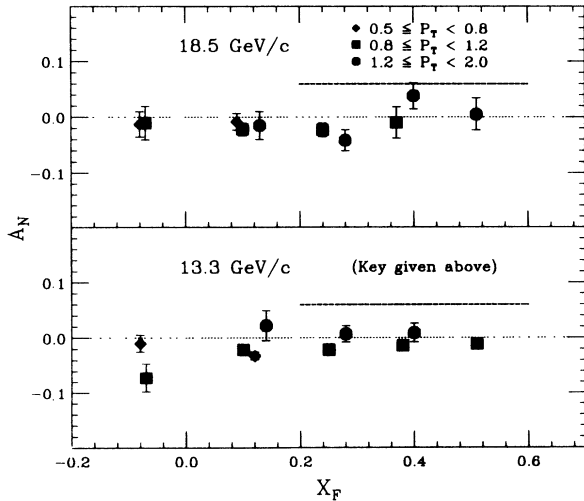


FIG. 9. Analyzing power of Λ data as a function of x_F . For clarity in viewing, data points with $0.8 \leq p_T < 1.2$ GeV/c have been shifted to the left by $x_F = 0.02$. The dashed line at $A_N = 0.06$ is the DM prediction corrected for the presence of Λ from Σ^0 decay.

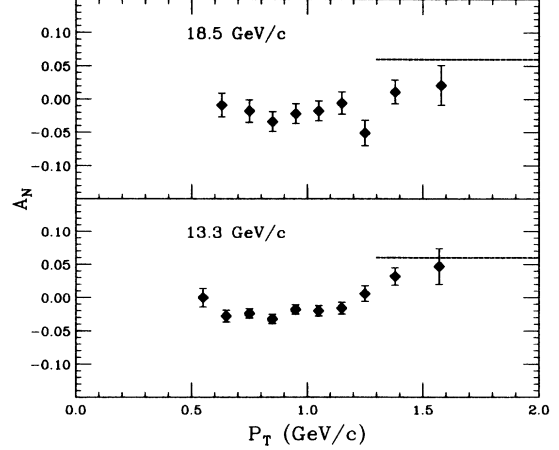


FIG. 10. Λ analyzing power as a function of p_T only. The dashed line at $A_N = 0.06$ is the DM prediction corrected for the presence of Λ from Σ^0 decay.

a value of one implies maximum polarization transfer. The following method used to calculate D_{NN} gives a result independent of the detector efficiency $E(\theta^*)$, since efficiency does not change between “spin-up” and “spin-down” beams. We start with a modified form of Eq. (1):

$$N^\mp(\theta^*) = \left[\frac{d\sigma}{d\Omega} \right]^\mp (1 + \alpha P_\Lambda^\mp \cos\theta^*) E(\theta^*). \quad (11)$$

Then using

$$\left[\frac{d\sigma}{d\Omega} \right]^\mp = \left[\frac{d\sigma}{d\Omega} \right]^0 (1 \mp P_B A_N) \quad (12)$$

and

$$P_\Lambda^\mp = \frac{P_\Lambda^0 \mp P_B D_{NN}}{1 \mp P_B A_N} \quad (13)$$

both of which can be derived from Eqs. (19)–(21), we get

$$N^\mp(\theta^*) = \left[\frac{d\sigma}{d\Omega} \right]^0 (1 \mp P_B A_N) E(\theta^*) \times \left[1 + \frac{(P_\Lambda^0 \mp P_B D_{NN}) \alpha \cos\theta^*}{1 \mp P_B A_N} \right]. \quad (14)$$

The superscript zero indicates measurements made with an unpolarized beam. $E(\theta^*)$ and $d\sigma/d\Omega$ cancel out when we calculate

$$B(\theta^*) = \frac{N^+(\theta^*) - N^-(\theta^*)}{N^+(\theta^*) + N^-(\theta^*)} \quad (15)$$

$$= \frac{P_B A_N + P_B D_{NN} \alpha \cos\theta^*}{1 + \alpha P_\Lambda \cos\theta^*} \quad (16)$$

from which D_{NN} can be extracted. The data is divided into 50 bins of $\cos\theta^*$ between -1 and $+1$. $B_i(\theta^*)$ and consequently $(D_{NN})_i$ are calculated independently for each bin $i=1,50$. D_{NN} is finally obtained by taking the mean of the $(D_{NN})_i$ weighting by the number of events in

each bin. The final results for D_{NN} as a function of x_F are shown in Fig. 11 and Table I. There is no significant deviation from zero implying that the spin of the Λ is not dependent on the spin of the incident proton.

The measurement of a nonzero beam polarization in the horizontal transverse direction raised concern that Λ 's might be produced asymmetrically about the horizontal plane and that this would lead to a false polarization measurement. However, Monte Carlo events generated with an asymmetry 0.0036 (using $P_B=0.18$ and $A_N=0.02$) showed no change in Λ polarization.

We also measured D_{SS} (by the same method used for D_{NN}) and found it to be -0.020 ± 0.016 .

C. Comparison with theory

The DM model⁴ provides a comprehensive set of predictions for hyperon-polarization parameters and is in fairly good agreement with existing data²⁴ taken with unpolarized beams. It has perfect success at predicting the sign of the polarization and can accommodate the observed magnitudes with perhaps a few discrepancies. The model classifies production processes into two types according to whether the final-state particle is composed of (a) two valence quarks (diquark) from the beam particle and a single quark from the sea (*VVS* recombination, e.g., $p \rightarrow \Lambda$ or $p \rightarrow \Sigma^0$) or (b) a single valence quark from the beam particle and a diquark from the sea (*VSS* recombination, e.g., $p \rightarrow \Xi^-$). [Produced particles which have no quarks in common with the beam particle are predicted (and observed) to show no polarization effects.] It is assumed that the quark or diquark transferred from the beam particle to the final-state particle preserves its spin state in the process. Also, the transition matrix element $\langle f | T | i \rangle$ is assumed to factorize into two subamplitudes for valence-diquark (or -quark) transfer and sea-quark (or -diquark) production for *VVS* (or *VSS*) processes. These are shown in Fig. 12. Spin dependence is incorporated into the theory by a simple parametrization of these amplitudes (see Fig. 12) involving small positive parameters ϵ , ϵ' , δ , and δ' . The signs are assigned such that it is more probable for a sea quark (or diquark) to recombine with spin down than with spin up, and vice versa for valence quarks (or diquarks). The quark spins are recom-

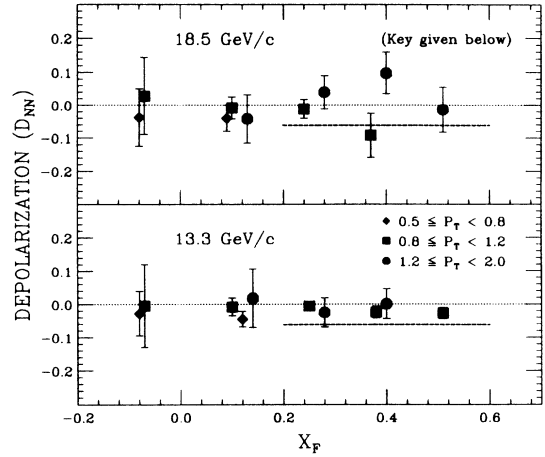


FIG. 11. Depolarization (D_{NN}) of Λ data as a function of x_F . For clarity in viewing, data points with $0.8 \leq p_T < 1.2$ GeV/c have been shifted to the left by $x_F=0.02$. The dashed line at $D_{NN} = -0.062$ is the DM prediction corrected for the presence of Λ from Σ^0 decay.

binned into hadrons according to static SU(6) wave functions.

This framework allows one to make predictions without necessarily adopting any particular mechanism for producing the polarization effects at the quark level. Note that DM themselves do not differentiate between ϵ and ϵ' or between δ and δ' . We have made this generalization because there does not seem to be any *a priori* reason for the subamplitudes of processes (a) and (d) and processes (b) and (c) to have identical spin asymmetries. In fact, comparison of $p \rightarrow \Lambda$ and $K^- \rightarrow \Lambda$ data suggests that ϵ' is significantly larger than ϵ .

The calculation of spin observables in the DM framework is best illustrated by an example. Consider the transition amplitude for the process $p \uparrow \rightarrow \Xi^- \uparrow$. The transferred d quark can have either spin up or spin down depending on whether the ss diquark is produced in an $S, M=1, 0$ or $S, M=1, 1$ state. [The ss diquark does not occur in $S, M=0, 0$ in the Ξ^- SU(6) wave function.] Therefore, we get

$$\begin{aligned} \langle \Xi^- \uparrow | T | p \uparrow \rangle &= C[\Xi^- \uparrow = d \uparrow (ss)_{10}] C[p \uparrow = d \uparrow (uu)_{10}] B'_\uparrow A'_{10} + C[\Xi^- \uparrow = d \downarrow (ss)_{11}] C[p \uparrow = d \downarrow (uu)_{11}] B'_\downarrow A'_{11} \\ &= \left(\frac{1}{3}\right) \left(-\frac{1}{3}\right) B'_\uparrow A'_{10} + \left[\frac{-\sqrt{2}}{3}\right] \left[\frac{\sqrt{2}}{3}\right] B'_\downarrow A'_{11}, \end{aligned} \quad (17)$$

where $C[\Xi^- \uparrow = d \uparrow (ss)_{10}]$ is proportional to the overlap between the $\Xi^- \uparrow$ SU(6) wave function and a state $|d \uparrow (ss)_{10}\rangle$. The transition rate $W_{fi} = |\langle f | T | i \rangle|^2$ ($f, i =$ spins of the final, initial baryons) is calculated assuming that amplitudes representing different spin configurations at the quark/diquark level will add incoherently. Hence, for $p \uparrow \rightarrow \Xi^- \uparrow$ we find

$$\begin{aligned} W_{\uparrow\uparrow} &= \frac{1}{81} |B'_\uparrow|^2 |A'_{10}|^2 + \frac{4}{81} |B'_\downarrow|^2 |A'_{11}|^2 \\ &= \frac{1}{81} A' B' [(1 + \epsilon') + 4(1 - \epsilon')(1 - \delta')]. \end{aligned} \quad (18)$$

The other W_{fi} 's are calculated similarly, and the polarization observables are given by

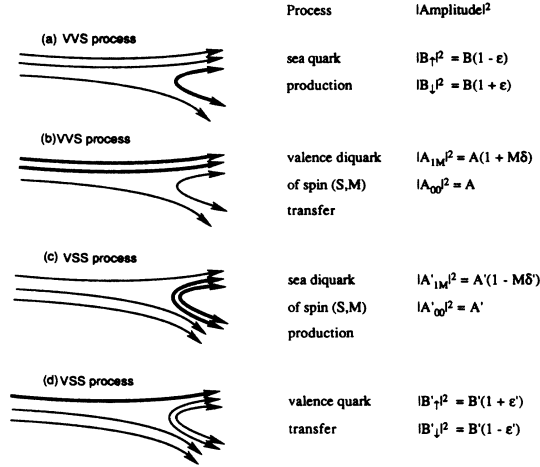


FIG. 12. Association between the various quark transfer/production processes and their corresponding amplitudes in the DeGrand and Miettinen model.

$$P = \frac{(W_{\uparrow\uparrow} + W_{\uparrow\downarrow}) - (W_{\downarrow\downarrow} + W_{\downarrow\uparrow})}{W_{\uparrow\uparrow} + W_{\uparrow\downarrow} + W_{\downarrow\downarrow} + W_{\downarrow\uparrow}}, \quad (19)$$

$$A_N = \frac{(W_{\uparrow\uparrow} + W_{\downarrow\uparrow}) - (W_{\downarrow\downarrow} + W_{\uparrow\downarrow})}{W_{\uparrow\uparrow} + W_{\uparrow\downarrow} + W_{\downarrow\downarrow} + W_{\downarrow\uparrow}}, \quad (20)$$

$$D = \frac{(W_{\uparrow\uparrow} + W_{\downarrow\downarrow}) - (W_{\uparrow\downarrow} + W_{\downarrow\uparrow})}{W_{\uparrow\uparrow} + W_{\uparrow\downarrow} + W_{\downarrow\downarrow} + W_{\downarrow\uparrow}}. \quad (21)$$

The parameters ϵ , ϵ' , δ , δ' can be functions of x_F and p_T . Nevertheless, there is still considerable predictive power in the model. In particular, because $W_{\uparrow\uparrow} = W_{\downarrow\downarrow}$ ($\epsilon \rightarrow -\epsilon, \delta \rightarrow -\delta$) and $W_{\uparrow\downarrow} = W_{\downarrow\uparrow}$ ($\epsilon \rightarrow -\epsilon, \delta \rightarrow -\delta$), the D_{NN} predicted by the model is parameter-free. This provides a test of the use of SU(6) wave functions and the as-

sumption that one can describe the process at the quark level. A list of predictions for various inclusive processes appears in Table II, adapted from a table in Ref. 4. Several asymmetries for pseudoscalar-meson production processes, which involve only the B, B' subamplitudes as in (a) and (d) of Fig. 12 have been included. As noted by DM in Ref. 4, these predictions are in fair agreement with experimental data on P if $\epsilon = \epsilon' = \delta = \delta' \simeq 0.15-0.3$. (References to these measurements are given in the Table II.) However, the large polarizations observed for $K^- \rightarrow \Lambda$ and $K^+ \rightarrow \bar{\Lambda}$ suggest that ϵ' may be a factor of 2 or 3 larger than ϵ . This possibility is compatible with the $p \rightarrow \Sigma^+$, $p \rightarrow \Xi^-$, and $p \rightarrow \Xi^0$ data if one takes $\delta' \simeq 0$.

Turning now to the $p \rightarrow \Lambda$ process measured in the present experiment we note that the DM model predicts $A_N = 0$ and $D_{NN} = 0$. This is easily understood since the ud diquark transferred from the proton is always in a spin-0 state; therefore, the Λ has no memory of the proton spin. However, this simple prediction is slightly modified by two complications: (a) some Λ 's may be produced by a subdominant VSS process, and (b) some Λ 's arise indirectly, from Σ^0 decay.

(a) If we perform the DM calculations allowing both VVS and VSS processes to contribute to Λ production, we still find $D_{NN} = 0$. A nonzero asymmetry

$$A_N = \frac{1}{6} \left[\frac{A'B'}{AB} \right] (\delta' + 2\epsilon') \quad (22)$$

does arise from the subdominant VSS terms. Using data on the production ratio of Σ^+ (VVS) to Σ^- (VSS) we can estimate that $A'B'/AB \simeq 0.08$ at $x_F \simeq 0.5$ giving an A_N of less than 1%. We can, therefore, ignore this effect.

(b) Since the experiment does not distinguish direct Λ 's from those arising from Σ^0 decay, we have to take this into account in the theoretical prediction. If the production ratio of Σ^0 's to direct Λ 's is denoted by n then the predicted asymmetry is

TABLE II. Spin-observable predictions using method of DeGrand and Miettinen (Ref. 4).

Reaction	P	A	D_{NN}	Reference
$p \rightarrow \Lambda$	$-\epsilon$	0	0	1, 2, and 17
$p \rightarrow \Sigma^+$	$\frac{1}{3}\epsilon + \frac{2}{3}\delta$	$\frac{2}{3}(\epsilon + \delta)$	$\frac{2}{3}$	6
$p \rightarrow \Sigma^0$	$\frac{1}{3}\epsilon + \frac{2}{3}\delta$	$\frac{2}{3}(\epsilon + \delta)$	$\frac{2}{3}$	7
$p \rightarrow \Sigma^-$	$\frac{2}{3}\epsilon' - \frac{1}{6}\delta'$	$-\frac{1}{3}\epsilon' - \frac{1}{18}\delta'$	$-\frac{2}{9}$	8
$p \rightarrow \Xi^-$	$-\frac{1}{3}\epsilon' - \frac{2}{3}\delta'$	$-\frac{1}{3}\epsilon' - \frac{2}{9}\delta'$	$\frac{1}{9}$	10
$p \rightarrow \Xi^0$	$-\frac{1}{3}\epsilon' - \frac{2}{3}\delta'$	$\frac{2}{3}\epsilon' + \frac{4}{9}\delta'$	$-\frac{2}{9}$	9
$p \rightarrow \pi^+$ or K^+		$\frac{2}{3}(\epsilon + \epsilon')$		28
$p \rightarrow \pi^-$ or K^0		$-\frac{1}{3}(\epsilon + \epsilon')$		27 and 28
$K^- \rightarrow \Lambda$	ϵ'			5
$K^+ \rightarrow \bar{\Lambda}$	ϵ'			29
$K^- \rightarrow \Sigma^-, \Sigma^0, \text{ or } \Sigma^+$	$-\frac{1}{3}\epsilon' - \frac{2}{3}\delta'$			
$K^- \rightarrow \Xi^-$	$\frac{2}{3}\epsilon' - \frac{1}{6}\delta'$			24
$\pi^+ \rightarrow \Lambda$	$-\frac{1}{2}\delta'$			
$\pi^- \rightarrow \Lambda$	$-\frac{1}{2}\delta'$			30

$$A_N = \frac{n}{n+1} A_N(\Sigma^0) = \frac{n}{n+1} \frac{2}{3} (\epsilon + \delta). \quad (23)$$

Also, because in $\Sigma^0 \rightarrow \Lambda$ decay the Λ acquires $-\frac{1}{3}$ of the polarization of the Σ^0 , the depolarization parameter is given by

$$D_{NN} = \left[\frac{n}{n+1} \right] \left[\frac{-1}{3} \right] D_{NN}(\Sigma^0) = \frac{-2}{9} \frac{n}{n+1} \quad (24)$$

since $D_{NN}(\Sigma^0) = \frac{2}{3}$. The observed value for polarization is also altered to

$$P_\Lambda^{\text{obs}} = \left[\frac{1}{1+n} \right] P_\Lambda + \left[\frac{n}{n+1} \right] \left[\frac{-1}{3} \right] P_{\Sigma^0}. \quad (25)$$

The experimentally observed value for n is 0.386 ± 0.041 (Ref. 22) and so we expect $D_{NN} \simeq -0.06$ and $A_N \simeq 0.06$ (for $\epsilon \simeq \delta \simeq 0.15$). These corrections to the predicted A_N and D_{NN} values are shown by the dashed lines in Figs. 9–11. There is fair agreement between experiment and theory except that at lower p_T values A_N seems to be slightly negative instead of slightly positive as expected. When substituting n in our expression for P_Λ^{obs} we get $P_\Lambda^{\text{obs}} = 0.72P_\Lambda - 0.09P_{\Sigma^0}$. The second term is small since $P_{\Sigma^0} = 0.28 \pm 0.13$ (Ref. 7). Therefore, the main effect is the dilution of the true polarization by the less polarized Λ 's from Σ^0 decay.

IV. K_S AND $\bar{\Lambda}$

A. K_S

Although the experiment was conceived primarily for the detection of Λ 's, the K_S 's (discarded as background earlier) proved numerous enough to enable a measurement of A_N in their production. They were isolated by (a) application of vertex and target cuts and (b) removal of all events with $1104 \text{ MeV}/c^2 < m_\Lambda < 1128 \text{ MeV}/c^2$. These conditions yielded 17 000 (33 000) events with $483 \text{ MeV}/c^2 < m_{K_S} < 513 \text{ MeV}/c^2$ at 13.3 (18.5) GeV/ c roughly between $x_F - 0.5 - 0.5$ and with $p_T \simeq 1 \text{ GeV}/c$ (Fig. 13). The observed slope of the $\cos\theta^*$ distribution for the K_S decay products is consistent with zero as it should be since the K_S is a spinless particle. Our results for A_N as a function of p_T are shown in Fig. 14 and listed in Table III. When averaged over all p_T we measured $\langle A \rangle = -0.094 \pm 0.012$ (-0.076 ± 0.015) for the 13.3 (18.5) GeV/ c sample.

To calculate the expected A_N for K_S production we must allow for the fact that the K_S can be produced either as K^0 or as \bar{K}^0 , or it can arise as a decay product of K^{*+} (892 MeV/ c^2) or K^{*0} (892 MeV/ c^2). Since K^{*-} production is a factor of 5 less than K^{*+} at 18 GeV/ c (Ref. 25), we may ignore K^{*-} and \bar{K}^{*0} , contributions. Thus, we have

$$A_N(K_S) = \frac{A_N(K^0) + A_N(\bar{K}^0)n_1 + A_N(K^{*+})\frac{2}{3}n_2 + A_N(K^{*0})\frac{1}{3}n_3}{1 + n_1 + \frac{2}{3}n_2 + \frac{1}{3}n_3}, \quad (26)$$

where n_1, n_2, n_3 are, respectively, the production ratios of \bar{K}^0, K^{*+} , and K^{*0} relative to direct K^0 's. The factors $\frac{2}{3}$ and $\frac{1}{3}$ included above correspond to the branching ratios for $K^{*+} \rightarrow K^0\pi^+$ and $K^{*0} \rightarrow K^0\pi^0$, respectively. The DM model gives $A_N(K^0) = -\frac{1}{3}(\epsilon + \epsilon')$, from Table II, and $A_N(\bar{K}^0) = 0$, since the \bar{K}^0 has no quarks in common with the proton. Calculating $A_N(K^{*+})$ and $A_N(K^{*0})$ in the DM model we find

$$A_N(K^{*+}) = -\frac{2}{9}\epsilon + \frac{2}{3}\epsilon', \quad (27)$$

$$A_N(K^{*0}) = \frac{1}{9}\epsilon - \frac{1}{3}\epsilon'. \quad (28)$$

The production ratio $n_1 \equiv \sigma(\bar{K}^0)/\sigma(K^0)$ cannot be directly obtained from available experimental data. However, we can relate it to $\sigma(K^-)/\sigma(K^+)$ which has been measured to be $\simeq \frac{1}{3}$ at 24 GeV/ c incident beam momentum²⁶ as follows: In the DM picture of fast-forward meson production $\sigma(K^0)$ should be one-half $\sigma(K^+)$ since the incident proton contains two u quarks but only one d quark. Assuming that $\sigma(\bar{K}^0) \simeq \sigma(K^-)$ since both are produced purely from sea quarks, we conclude that $n_1 \equiv \sigma(\bar{K}^0)/\sigma(K^0) \simeq 2\sigma(K^-)/\sigma(K^+) \simeq \frac{2}{3}$. Next, for our calculation of n_2 we note that

$\sigma(K^{*+})/\sigma(\text{direct } K^0)$ has been measured to be $\simeq \frac{1}{2}$ for pp interactions at 18 GeV/ c (Ref. 25). The relative detector efficiency between K^0 and K^{*+} must also be taken into account, since the pion from $K^{*+} \rightarrow K^0\pi^+$ can pass through S4 and thus, veto the trigger. This efficiency was determined by requiring Monte Carlo-generated K^0 and

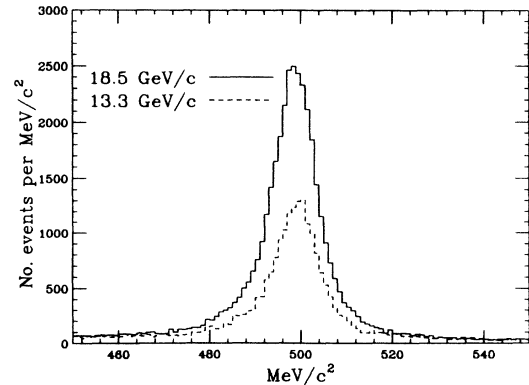


FIG. 13. Invariant mass of purified K_S sample under the hypothesis $K_S \rightarrow \pi^+\pi^-$.

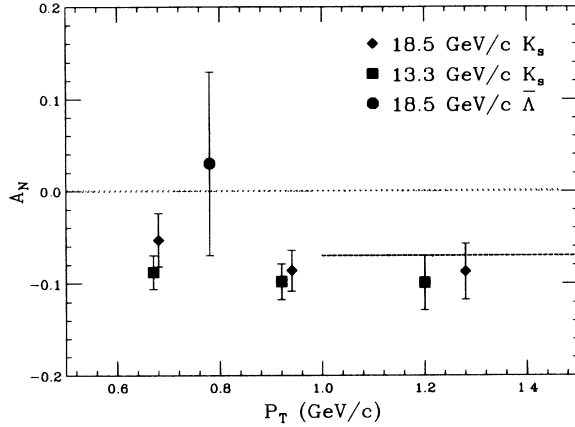


FIG. 14. Analyzing power of K_S and $\bar{\Lambda}$. The dashed line at $A_N = -0.7$ is the DM prediction for A_N of K_S .

K^{*+} events to satisfy the trigger conditions in the detector. We found that the π^+ vetoed the trigger 20% of the time, giving a relative efficiency 0.8. This gave

$$n_2 \equiv (0.8)\sigma(K^{*+})/\sigma(\text{direct } K^0) \simeq \frac{1}{2}(0.8) = \frac{2}{5}.$$

Finally since $\sigma(K^{*0})/\sigma(K^{*+})$ is $\frac{1}{2}$ in the DM model just as for the K^0 to K^+ ratio mentioned above, we expect $n_3 \simeq \frac{1}{2}\sigma(K^{*+})/\sigma(\text{direct } K^0) \simeq \frac{1}{4}$. Combining all this information we obtain

$$A_N \simeq -0.19\epsilon - 0.09\epsilon'. \quad (29)$$

For reasonable values of ϵ, ϵ' (e.g., $\epsilon \simeq 0.15$, $\epsilon' \simeq 3\epsilon$ would give $A_N \simeq -7\%$) this prediction accords quite well with the observed asymmetry shown in Fig. 14.

Our values of A_N contrast rather sharply with an earlier measurement of $A_N = -0.52 \pm 0.12$ (Ref. 27), in which 346 events were obtained from using 6 GeV/c polarized protons ($\sqrt{s} = 3.627$ GeV) incident on a hydrogen target. The observed difference could be due to (i) decrease of A_N with beam energy, a phenomenon which has

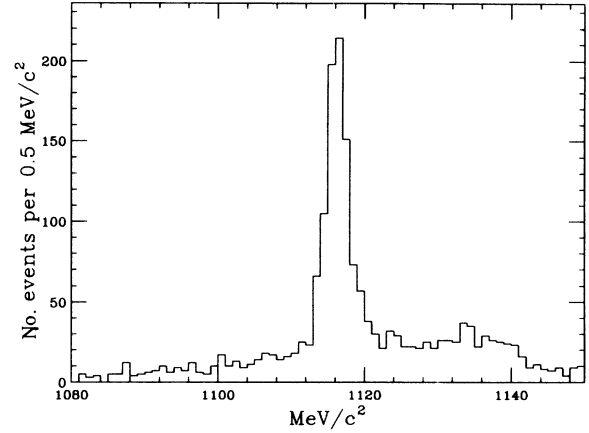


FIG. 15. Invariant mass of purified $\bar{\Lambda}$ sample in $\bar{p}\pi^+$ hypothesis.

been seen in other reactions, or (ii) the influence on A_N of the larger fraction of \bar{K}^0 's and K^{*} 's in our data which tend to reduce the magnitude of the asymmetry, as discussed above. At 6 GeV/c \bar{K}^0 and K^* production are suppressed by the close proximity to (mass-energy) threshold for even the lowest-energy exclusive states.

B. $\bar{\Lambda}$

A small sample of $\bar{\Lambda}$'s was also obtained in this experiment. These were isolated by (a) requiring the magnitude of momentum to be greater for the negative decay particle than for the positive particle which is, true for all $\bar{\Lambda}$ with $p_{\text{lab}} > 300$ MeV/c, (b) imposing vertex and target cuts, and (c) discarding events with $483 \text{ MeV}/c^2 < m_{K_S} < 513 \text{ MeV}/c^2$. A was measured only for the 18.5 GeV/c (Fig. 15) sample which had 807 $\bar{\Lambda}$'s with $1113 \text{ MeV}/c^2 < m_{\bar{\Lambda}} < 1119 \text{ MeV}/c^2$. Our statistics were insufficient at 13.3 GeV/c. The value of $A_N = 0.03 \pm 0.10$ (Fig. 14) is consistent with the DM prediction of zero.

TABLE III. Analyzing power of K_S at 13.3 and 18.5 GeV/c.

x_F	$\langle x_F \rangle$	p_T (GeV/c)	$\langle p_T \rangle$ (GeV/c)	A
18.5 GeV/c				
-0.70 to -0.06	-0.22		0.82	-0.088 ± 0.026
-0.06 to 0.12	0.03		0.97	-0.053 ± 0.026
0.12 to 0.60	0.23		1.08	-0.090 ± 0.027
	-0.16	0.3 to 0.8	0.68	-0.053 ± 0.029
	0.02	0.8 to 1.1	0.94	-0.086 ± 0.022
	0.0	1.1 to 1.8	1.28	-0.087 ± 0.030
13.3 GeV/c				
-0.70 to -0.06	-0.21		0.72	-0.091 ± 0.021
-0.06 to 0.14	0.04		0.88	-0.064 ± 0.021
0.14 to 0.70	0.29		0.96	-0.120 ± 0.020
	-0.08	0.3 to 0.8	0.67	-0.088 ± 0.018
	0.11	0.8 to 1.06	0.92	-0.098 ± 0.019
	0.06	1.06 to 1.6	1.20	-0.099 ± 0.029

V. SUMMARY AND CONCLUSIONS

We have used the Brookhaven polarized proton beam to study inclusive production of Λ particles at moderate p_T . The measurement of P_Λ showed good agreement with data taken in other experiments that used unpolarized beam. A_N and D_{NN} were both found to be approximately zero, in reasonable agreement with the DeGrand and Miettinen (DM) model of hyperon polarization. The value obtained for A_N is slightly lower than what we expect from DM but approaches the prediction at the highest p_T . Our value of $D_{NN} \simeq 0$ supports the picture of the beam proton contributing only a spinless (ud) quark pair to the Λ regardless of the beam polarization. The DM model seems to overestimate the magnitude of D_{NN} slightly, predicting $D_{NN} = -0.06$ when the effect of Λ 's arising from Σ^0 decay is included. There is a hint that the model may not be correct; therefore, a comparison between theory and experiment for a large nonzero D_{NN} measurement (e.g., Σ^+ or Σ^0 production) would perhaps shed light on the situation.

The measurement of A_N for K_S gives $A_N \simeq 0.1$, independent of x_F . The DM model agrees well with this in the forward x_F region when we account for K_S 's arising from K^0 , \bar{K}^0 , and the decays of K^* 's. In the backward-scattered region, however, the DM model predicts zero since the target is unpolarized. Further experiments in hyperon polarization with polarized beams should play an important part in determining the role of valence quarks as spin carriers in hadrons.

ACKNOWLEDGMENTS

We thank Dr. W. Glenn, Dr. K. Foley, and Dr. A. Etkin as well as the staffs of the MPS group and the AGS department. For the commissioning and running of the polarized beam we are indebted to Professor Alan Krisch and Dr. L. Ratner. We are also grateful to Dr. L. Trueman for providing the computer resources to analyze the data and to the staffs of the CSCF and OLDF for their consideration. This work was performed with the support of the United States Department of Energy.

-
- ¹G. Bunce *et al.*, Phys. Rev. Lett. **36**, 1113 (1976).
²K. Raychaudhuri *et al.*, Phys. Lett. **90B**, 319 (1980).
³B. Andersson, G. Gustafson, and G. Ingelman, Phys. Lett. **85B**, 417 (1979).
⁴T. A. DeGrand and H. I. Miettinen, Phys. Rev. D **23**, 1227 (1981); **24**, 2419 (1981); **31**, 661(E) (1985); T. A. DeGrand, J. Markkanen, and H. I. Miettinen, *ibid.* **32**, 2445 (1985).
⁵S. A. Gourlay *et al.*, Phys. Rev. Lett. **56**, 2244 (1986).
⁶C. Wilkinson *et al.*, Phys. Rev. Lett. **46**, 803 (1981).
⁷E. C. Dukes *et al.*, Phys. Lett. B **192**, 135 (1987).
⁸L. Deck *et al.*, Phys. Rev. D **28**, 1 (1983).
⁹K. Heller *et al.*, Phys. Rev. Lett. **51**, 2025 (1983).
¹⁰R. Rameika, Ph.D. thesis, Rutgers University, 1981.
¹¹O. E. Overseth and R. F. Roth, Phys. Rev. Lett. **19**, 391 (1967).
¹²*Higher Energy Polarized Beams*, proceedings of the Ann Arbor Workshop, 1978, edited by A. D. Krisch and A. J. Salt-house (AIP Conf. Proc. No. 42) (AIP, New York, 1978), p. 142.
¹³B. E. Bonner *et al.*, Phys. Rev. Lett. **58**, 447 (1987).
¹⁴L. G. Ratner *et al.*, IEEE Trans. Nucl. Sci. **32**, 2635 (1985).
¹⁵D. Cohen, Rev. Sci. Instrum. **33**, 161 (1962).
¹⁶D. G. Crabb *et al.*, IEEE Trans. Nucl. Sci. **30**, 4 (1983); **30**, 2176 (1983); G. R. Court *et al.*, Phys. Rev. Lett. **57**, 507 (1986).
¹⁷K. Heller *et al.*, Phys. Rev. Lett. **51**, 2025 (1983); S. Erhan *et al.*, Phys. Lett. **82B**, 301 (1979).
¹⁸S. Ozaki, Brookhaven National Laboratory Report Nos. BNL-17873 and BNL-25311, 1979 (unpublished).
¹⁹S. Eiseman *et al.*, Brookhaven National Laboratory Report No. BNL-20784-mc (microfiche) (unpublished).
²⁰G. G. Ohlsen and P. W. Keaton, Jr., Nucl. Instrum. Methods **109**, 41 (1973).
²¹C. Geweniger *et al.*, Phys. Lett. **57B**, 193 (1975).
²²M. W. Sullivan *et al.*, Phys. Rev. D **36**, 674 (1987).
²³S. R. Tonse, Ph.D. thesis, Rice University, 1988.
²⁴P. A. Baker *et al.*, Phys. Rev. Lett. **40**, 678 (1978); J. Bensing-inger *et al.*, Nucl. Phys. **B252**, 561 (1985); Bunce (Ref. 1); Raychaudhuri (Ref. 2); Wilkinson *et al.* (Ref. 6); Dukes *et al.* (Ref. 7); Deck *et al.* (Ref. 8); Heller *et al.* (Ref. 9); Rameika (Ref. 10); Heller *et al.* (Ref. 17); and Erhan *et al.* (Ref. 17).
²⁵H. Kichimi *et al.* Phys. Rev. D **20**, 37 (1979).
²⁶J. V. Allaby *et al.*, Report No. CERN 70-12, 1970 (unpublished).
²⁷R. L. Eisner *et al.* Nucl. Phys. **B123**, 361 (1977).
²⁸W. H. Dragoset *et al.*, Phys. Rev. D **18**, 3939 (1978).
²⁹I. V. Ajinenko *et al.*, Phys. Lett. **121B**, 183 (1983).
³⁰J. Bensing-inger *et al.*, Phys. Rev. Lett. **50**, 313 (1983).